

Supporting information

Revised model of the tissue factor pathway of thrombin generation: role of the feedback activation of FXI

Hari Hara Sudhan Lakshmanan^{1#}, Aldrich Estonilo², Stephanie E. Reitsma¹, Alexander R. Melrose¹, Jayaram Subramanian³, Tony J. Zheng¹, Jeevan Maddala⁴, Erik I. Tucker^{1,5}, David Gailani⁶, Owen J.T. McCarty¹, Patrick L. Journey^{2*} and Cristina Puy^{1*}

¹*Department of Biomedical Engineering, Oregon Health & Science University, Oregon, USA;*

²*Department of Biomedical Engineering, San José State University, California, USA;* ³*Enginuity Power Systems, Virginia, USA;* ⁴*Department of Chemical and Biomedical Engineering, West Virginia University, West Virginia, USA;* ⁵*Aronora, Inc., Portland, Oregon, USA;* ⁶*Department of Pathology, Microbiology and Immunology, Vanderbilt University, Nashville, USA.*

*Patrick L. Journey and Cristina Puy are co-senior authors

Correspondence:

Hari Hara Sudhan Lakshmanan
Department of Biomedical Engineering
Oregon Health and Science University
3303 SW Bond Ave.
Portland, OR 97239
E-mail: lakshmah@ohsu.edu

Table S1. Average initial plasma concentrations of enzymes and inhibitors

Species	Initial concentration (nM)
TF	Varied
FVII	10
TF-FVII	0
FVIIa	0.1
TF-FVIIa	0
FXa	0
FIIa (thrombin)	0
FX	160
TF-FVIIa-FX	0
TF-FVIIa-FXa	0
FIX	90
TF-FVIIa-FIX	0
FIXa	0
FII (prothrombin)	1400
FVIII	0.7
FVIIIa	0
FIXa-FVIIIa	0
FIXa-FVIIIa-FX	0
FVIIIa ₁	0
FVIIIa ₂	0
FV	20
FVa	0
FXa-FVa	0
FXa-FVa-FII	0
mFIIa (meizothrombin)	0
TFPI	2.5
FXa-TFPI	0
FVIIa-TF-FXa-TFPI	0
ATIII	3400
FXa-ATIII	0
mFIIa-ATIII	0
FIXa-ATIII	0
FIIa-ATIII	0
TF-FVIIa-ATIII	0
FXI	30
FXI-FIIa	0
FXIa	0
FXIa-FIX	0

Table S1. (continued)

Species	Initial concentration (nM)
C1-INH	2500
FXIa-C1-INH	0
FXIa-ATIII	0
FIXa-FX	0

FII – prothrombin, TF- Tissue factor, FV – coagulation factor V, FVII – coagulation factor VII, FVIII – coagulation factor VIII, FIX – coagulation factor IX, FX – coagulation factor X, FXI – coagulation factor XI, ATIII – antithrombin, TFPI – tissue factor pathway inhibitor, C1-INH – C1 inhibitor, FVIII₁ and FVIII₂ – trimeric forms of FVIIIa, mFIIa –meizothrombin. The activated forms of the coagulation factor are represented with ‘a’ added as the suffix, such as FIIa, FVIIa, FVIIIa, FIXa, FXa and FVa.

Table S2. Reactions and kinetic constants of the extended Hockin-Mann model

No.	Reactions	Kinetic constant	Units
1	$TF + FVII = TF-FVII$	1.7×10^5	$M^{-1}s^{-1}$
2	$TF-FVII = TF + FVII$	3.0×10^{-3}	s^{-1}
3	$TF + FVIIa = TF-FVIIa$	2.2×10^8	$M^{-1}s^{-1}$
4	$TF-FVIIa = TF + FVIIa$	3.1×10^{-5}	s^{-1}
5	$TF-FVIIa + FVII = TF-FVIIa + FVIIa$	4.4×10^5	$M^{-1}s^{-1}$
6*	$TF-FVIIa + TF-FVII = TF-FVIIa + TF-FVIIa$	4.4×10^5	$M^{-1}s^{-1}$
7	$FXa + FVII = FXa + FVIIa$	2.5×10^9	$M^{-1}s^{-1}$
8*	$FXa + TF-FVII = FXa + TF-FVIIa$	2.5×10^9	$M^{-1}s^{-1}$
9	$FIIa + FVII = FIIa + FVIIa$	2.3×10^4	$M^{-1}s^{-1}$
10*	$FIIa + TF-FVII = FIIa + TF-FVIIa$	2.3×10^4	$M^{-1}s^{-1}$
11	$TF-FVIIa + FX = TF-FVIIa-FX$	7.5×10^6	$M^{-1}s^{-1}$
12	$TF-FVIIa-FX = TF-FVIIa + FX$	5.2×10^{-1}	s^{-1}
13	$TF-FVIIa-FX = TF-FVIIa-FXa$	1.1×10^1	s^{-1}
14	$TF-FVIIa + FXa = TF-FVIIa-FXa$	2.2×10^7	$M^{-1}s^{-1}$
15	$TF-FVIIa-FXa = TF-FVIIa + FXa$	3.9×10^1	s^{-1}
16	$TF-FVIIa + IX = TF-FVIIa-IX$	2.7×10^7	$M^{-1}s^{-1}$
17	$TF-FVIIa-IX = TF-FVIIa + IX$	4.2×10^2	s^{-1}
18	$TF-FVIIa-IX = TF-FVIIa + FIXa$	1×10^1	s^{-1}
19	$FII + FXa = FIIa + FXa$	9.2×10^3	$M^{-1}s^{-1}$
20	$FIIa + FVIII = FIIa + FVIIIa$	2.5×10^7	$M^{-1}s^{-1}$
21	$FVIIIa + FIXa = FIXa-FVIIIa$	5×10^7	$M^{-1}s^{-1}$
22	$FIXa-FVIIIa = FVIIIa + FIXa$	2.8×10^{-3}	$M^{-1}s^{-1}$
23	$FIXa-FVIIIa + X = FIXa-FVIIIa-FX$	1.3×10^8	$M^{-1}s^{-1}$
24	$FIXa-FVIIIa-X = FIXa-FVIIIa + X$	1.0×10^{-3}	s^{-1}
25	$FIXa-FVIIIa-X = FIXa-FVIIIa + FXa$	4.2×10^1	s^{-1}
26	$FVIIIa = FVIIIa1 + FVIIIa2$	7.5×10^{-3}	s^{-1}
27	$FVIIIa1 + FVIIIa2 = FVIIIa$	2.1×10^4	$M^{-1}s^{-1}$
28	$FIXa-FVIIIa-FX = FVIIIa1 + FVIIIa2 + FX + FIXa$	1.4×10^{-4}	s^{-1}
29	$FIXa-FVIIIa = FVIIIa1 + FVIIIa2 + FIXa$	6.1×10^{-4}	s^{-1}
30	$FIIa + FV = FIIa + FVa$	2.3×10^7	$M^{-1}s^{-1}$
31	$FXa + FVa = FXa-FVa$	4.9×10^8	$M^{-1}s^{-1}$
32	$FXa-FVa = FXa + FVa$	3×10^{-1}	s^{-1}
33	$FXa-FVa + FII = FXa-FVa-FII$	2.5×10^7	$M^{-1}s^{-1}$
34	$FXa-FVa-FII = FXa-FVa + FII$	7.8×10^1	s^{-1}
35	$FXa-FVa-FII = FXa-FVa + mFIIa$	1.3×10^1	s^{-1}
36	$FXa-FVa + mFIIa = FXa-FVa + FIIa$	2.3×10^7	s^{-1}
37	$FXa + TFPI = FXa-TFPI$	2.2×10^7	$M^{-1}s^{-1}$
38	$FXa-TFPI = FXa + TFPI$	3.7×10^{-5}	s^{-1}

Table S2. (continued)

No.	Reactions	Kinetic constant	Units
39	$\text{TF-FVIIa-FXa} + \text{TFPI} = \text{TF-FVIIa-FXa-TFPI}$	1×10^7	$\text{M}^{-1}\text{s}^{-1}$
40	$\text{TF-FVIIa-FXa-TFPI} = \text{TF-FVIIa-FXa} + \text{TFPI}$	1×10^{-5}	s^{-1}
41	$\text{TF-FVIIa} + \text{FXa-TFPI} = \text{TF-FVIIa-FXa-TFPI}$	4.4×10^8	$\text{M}^{-1}\text{s}^{-1}$
42	$\text{FXa} + \text{ATIII} = \text{FXa-ATIII}$	1.2×10^3	$\text{M}^{-1}\text{s}^{-1}$
43	$\text{mFIIa} + \text{ATIII} = \text{mFIIa-ATIII}$	1×10^4	$\text{M}^{-1}\text{s}^{-1}$
44	$\text{FIXa} + \text{ATIII} = \text{FIXa-ATIII}$	7×10^2	$\text{M}^{-1}\text{s}^{-1}$
45	$\text{FIIa} + \text{ATIII} = \text{FIIa-ATIII}$	2.1×10^3	$\text{M}^{-1}\text{s}^{-1}$
46	$\text{TF-FVIIa} + \text{ATIII} = \text{TF-FVIIa-ATIII}$	3.3×10^2	$\text{M}^{-1}\text{s}^{-1}$
47*	$\text{FXI} + \text{FIIa} = \text{FXI-FIIa}$	5×10^7	$\text{M}^{-1}\text{s}^{-1}$
48*	$\text{FXI-FIIa} = \text{XI} + \text{FIIa}$	9.9	s^{-1}
49*	$\text{FXI-FIIa} = \text{FXIa} + \text{FIIa}$	1.1×10^{-4}	s^{-1}
50*	$\text{FXIa} + \text{FIX} = \text{FXIa-FIX}$	6.1×10^5	$\text{M}^{-1}\text{s}^{-1}$
51*	$\text{FXIa-IX} = \text{FXIa} + \text{IX}$	9.9×10^{-1}	s^{-1}
52*	$\text{FXIa-IX} = \text{FXIa} + \text{FIXa}$	1.1×10^{-1}	s^{-1}
53*	$\text{FXIa} + \text{ATIII} = \text{FXIa-ATIII}$	3.2×10^2	$\text{M}^{-1}\text{s}^{-1}$
54*	$\text{FXIa} + \text{C1-INH} = \text{FXIa-C1-INH}$	1.8×10^3	$\text{M}^{-1}\text{s}^{-1}$
55*	$\text{FIXa} + \text{FX} = \text{FIXa-FX}$	1×10^8	$\text{M}^{-1}\text{s}^{-1}$
56*	$\text{FIXa-FX} = \text{FIXa} + \text{FX}$	3.3×10^2	s^{-1}
57*	$\text{FIXa-FX} = \text{FIXa} + \text{FXa}$	3×10^{-3}	s^{-1}

Asterisk (*) denotes reactions that are newly added to the HM model in this study.

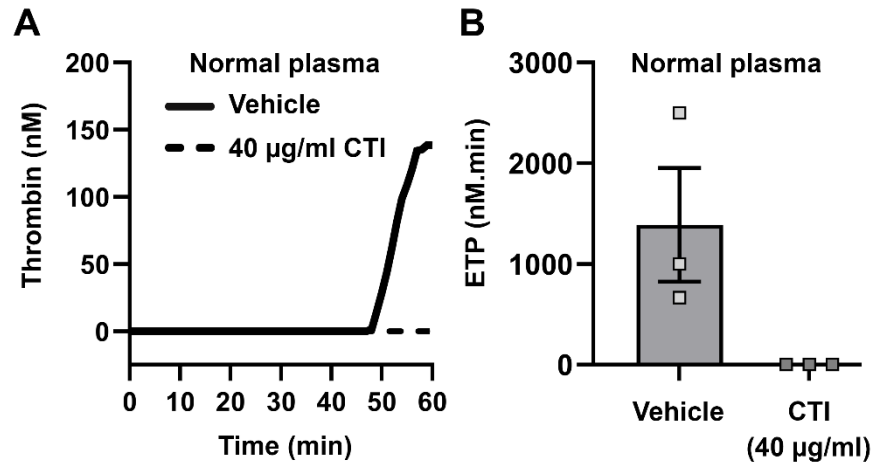


Fig S1: Validating the experimental concentration of CTI used in thrombin generation in plasma. (A) Thrombin generation in normal plasma supplemented with vehicle or 40 µg/ml CTI was initiated by adding CaCl₂. (B) ETP was estimated from the thrombin generation curves for each condition. Data are means ± SE (n = 3).

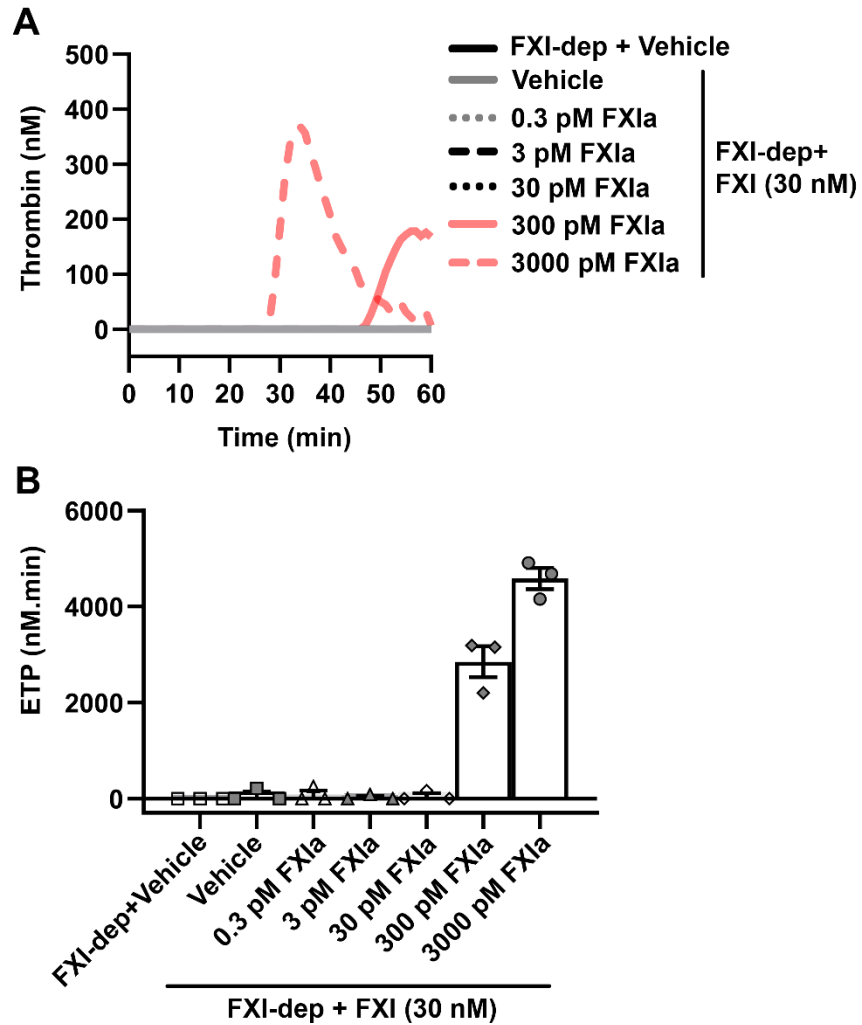


Fig S2: Effect of FXIa on thrombin generation in FXI-depleted plasma supplemented with FXI. (A) FXI-depleted plasma (FXI-dep) supplemented with 30 nM FXI or vehicle was incubated with increasing concentrations of FXIa (0-3000 pM) for 30 min. Thrombin generation was initiated by adding CaCl₂. (B) ETP for each condition was estimated from the thrombin generation curves. Data are means \pm SE (n = 3).

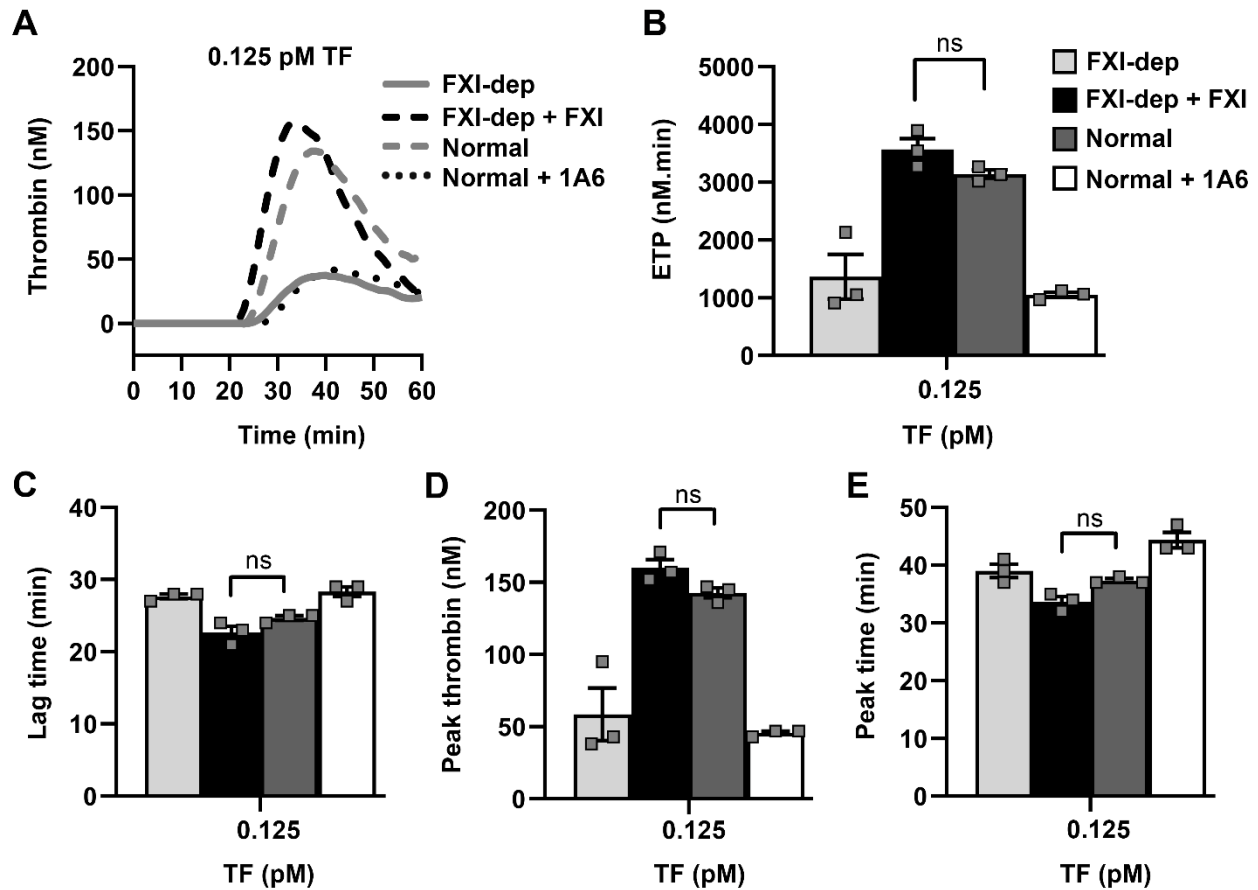


Fig S3: Comparison of TF-initiated thrombin generation in normal plasma with FXI-depleted plasma supplemented with FXI. (A) Thrombin generation in normal or FXI-depleted plasma (FXI-dep) supplemented with 30 nM FXI or vehicle was initiated by the addition of TF (0.125 pM) and CaCl₂. Normal plasma was supplemented with either vehicle or anti-FXI mAb, 1A6 (30 μg/ml). (B) ETP, (C) Lag time, (D) Peak thrombin and (E) Peak time were estimated from the thrombin generation curves for each condition in normal and FXI-dep plasma. Data are means ± SE (n = 3). ns – not significant.

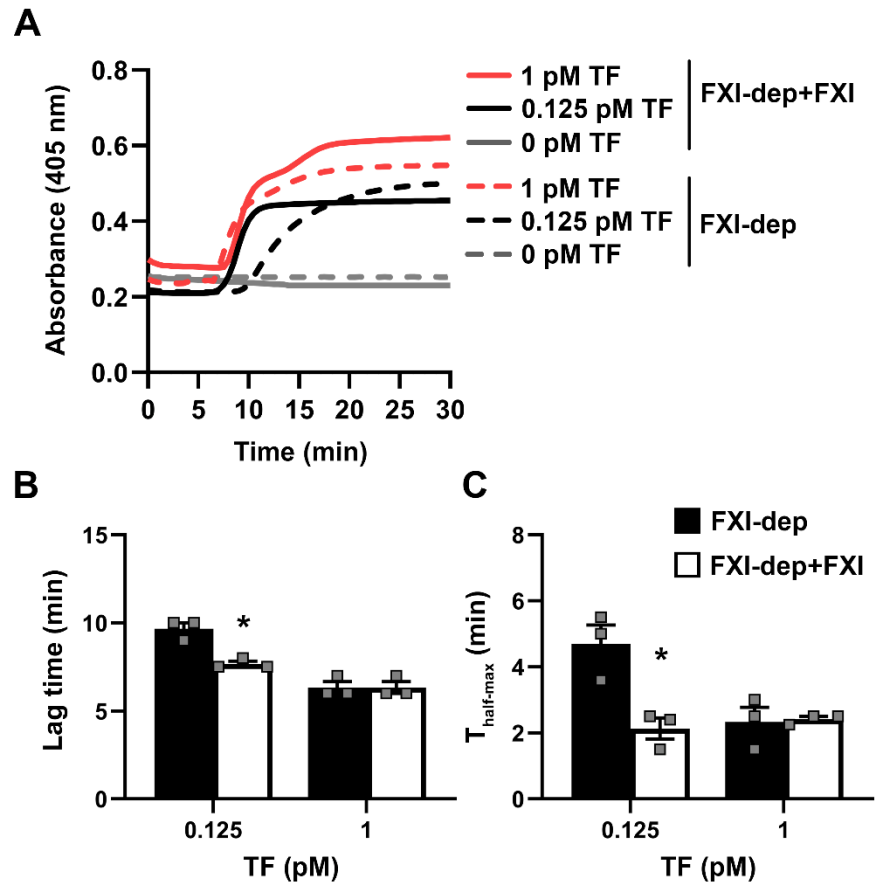


Fig S4: Effect of FXI on TF-initiated fibrin generation in FXI-depleted plasma. (A) FXI-depleted plasma (FXI-dep) was supplemented with 30 nM FXI or vehicle and fibrin generation was initiated by adding TF (0, 0.125 or 1 pM) and CaCl₂. Fibrin generation was measured through recording changes in absorbance at 405 nm due to change in turbidity of the plasma (B) Lag time – time to initiate fibrin generation and (C) $T_{\text{half-max}}$ – time to reach half-maximal fibrin generation were determined from the fibrin generation curves for each condition. Data are means \pm SE (n = 3). * P < 0.05 with respect to FXI-dep.

Supporting methods:

FXI-depleted plasma was incubated with vehicle or 30 nM FXI for 30 min and treated with 40 $\mu\text{g/ml}$ CTI. Post-incubation period the plasma (40 μl) is pipetted into a 96-well polystyrene plate and fibrin formation was initiated by adding 60 μl CaCl₂ (15mM) for all the experiments. TF (0.125 or 1 pM) was added in combination with CaCl₂ for select experiments. Fibrin generation was measured by monitoring turbidity at 405 nm every 30 seconds for 30 min using an Infinite M200 plate reader (TECAN, Switzerland). The time required to initiate fibrin formation as measured by the rapid change in absorbance is measured as the lag time and the time required for the turbidity of the solution to reach the half-maximal value was defined as $T_{\text{half-max}}$.

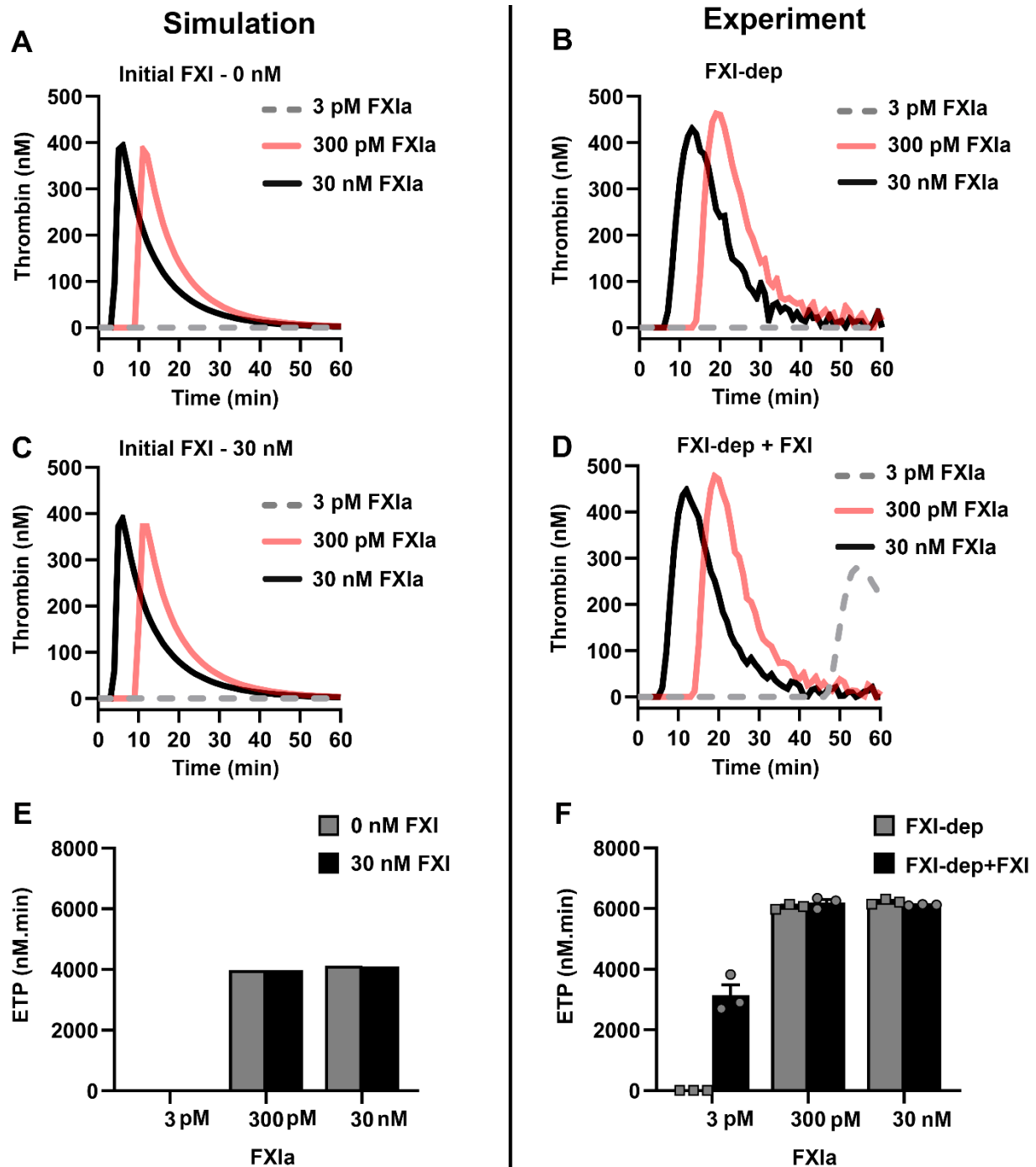


Fig S5: Comparison of *in silico* and *in vitro* FXIa-initiated thrombin generation in FXI-depleted plasma. Thrombin generation in plasma was simulated using the extended (ext.) Hockin-Mann (HM) model with the physiological concentrations of enzymes as described in methods, with 3 pM, 300 pM, or 30 nM FXIa and (A) 0 nM FXI or (C) 30 nM FXI. Thrombin generation in FXI-depleted plasma supplemented with (B) vehicle or (D) 30 nM FXI was initiated by adding 3 pM, 300 pM or 30 nM FXIa with CaCl₂. ETP estimated from the (E) simulations and (F) the experiments for each condition respectively. Experimental data are shown as means \pm SE (n = 3).

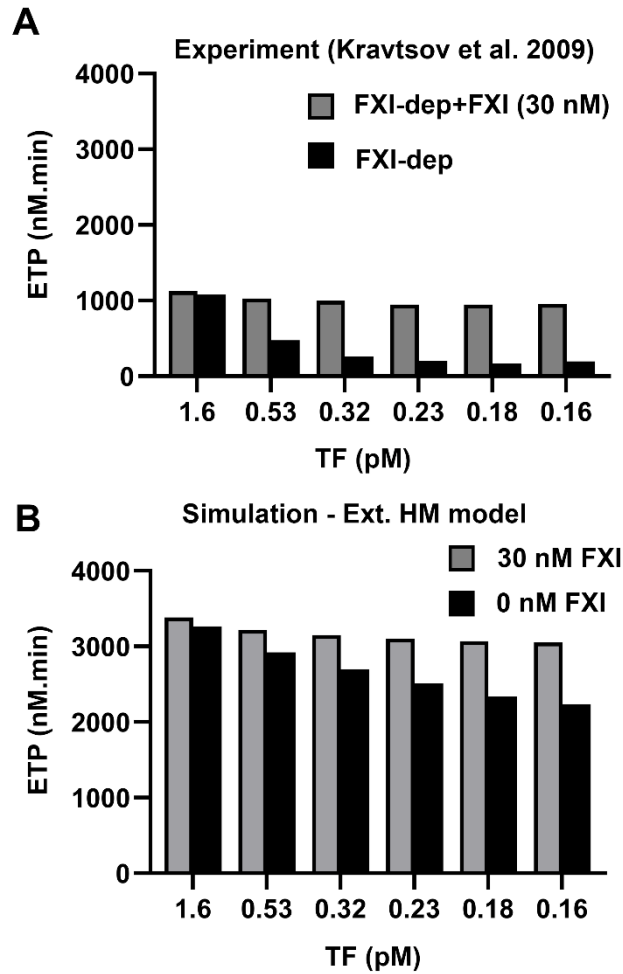


Fig S6: Comparison of ETP from TF-initiated thrombin generation from Kravtsov et al. (2009) with the ETP predicted using the ext. HM model. (A) ETP data from the TF-initiated thrombin generation experiments in FXI-deficient plasma in the presence or absence of 30 nM FXI as reported by Kravtsov et al. in Blood (2009), (B) ETP from simulations of thrombin generation using the ext.HM model. Simulations were initiated with physiological concentrations of enzymes and 30 or 0 nM FXI for select TF concentrations (1.6 - 0.16 pM).